Enhancement of the Magnetoelectric Effect Using the Dynamic Jahn-Teller Effect in a Transition-Metal Complex

Yasunao Otsuki,[1] Shojiro Kimura,[1] Satoshi Awaji,[1] and Motohiro Nakano[2]
[1]Institute for Materials Research, Tohoku University, Katahira 2-1-1, Sendai 980-8577, Japan
[2]Research Center for Thermal and Entropic Science, Graduate School of Science, Osaka University, Toyonaka 560-0043, Japan

(Received 6 August 2021; revised 19 November 2021; accepted 17 February 2022; published 15 March 2022)

In this Letter, a novel mechanism to enhance the magnetoelectric (ME) coupling between electric polarization and magnetism using the dynamic Jahn-Teller (JT) effect is demonstrated. Electric polarization of over 100 $\mu C/m^2$ is induced by the magnetic field owing to the second-order ME effect in the noncentrosymmetric transition metal complex [Mn^{III}(taa)]. This appearance of electric polarization does not require magnetic order in contrast to the linear ME effect in ME multiferroic materials. The value of the electric polarization is 1 order larger than that induced by the second-order ME effect, which originates from the p–d hybridization. Our calculation, taking into account the single-ion-type magnetic anisotropy originating from the spin-orbit interaction and ferrodistortive intermolecular interaction, verifies that the alignment of the JT distortion by the magnetic field results in the large electric polarization observed. Thus, our results provide a new method to gain strong ME coupling by tuning the atomic displacement using a magnetic field.

DOI: 10.1103/PhysRevLett.128.117601

The magnetoelectric (ME) effect has attracted much attention from the points of view of both fundamental and applied physics because of its various microscopic mechanisms and high potential for application in novel devices such as voltage-controllable magnetic memories [1,2]. To enable practical application of the ME effect, it is essential to strengthen the coupling between the electric polarization and magnetism. In many spin-driven ferroelectrics, in which ferroelectricity is induced by the magnetic order, the coupling occurs by the spin current [3,4] or p–d hybridization mechanism [5]. In these mechanisms, charge polarization because of the hybridization between the p and d orbitals is modulated by the spin-orbit interaction, resulting in ME coupling. However, to gain stronger ME coupling, usage of the electric dipole generated by atomic displacement is more advantageous than that by the hybridization of p–d orbitals. In fact, exchange striction, which causes substantial atomic displacements, is known to induce a spin-dependent electric polarization that is more than 1 order of magnitude larger than that induced by the spin current mechanism [6–9]. In this Letter, we propose a new method to achieve the strong ME effect by utilizing the dynamic Jahn-Teller (JT) effect, which efficiently couples an electric dipole by atomic displacement and spin.

The generation of the linear ME effect requires the breaking of both space inversion and time reversal symmetries. Therefore, ME multiferroic materials, in which the ferroelectricity and magnetic orders coexist, have been the main target of research. The effects of the cooperative JT distortion, which can be a source of ME multiferroicity [10] or an electronically polar state in a magnetic ordered system [11], have been also discussed. However, although the material is paramagnetic, an electric polarization can be induced owing to the second-order ME effect when its crystal symmetry is piezoelectric with no centrosymmetry [12–19]. The electric polarization $\boldsymbol{P}$ by the second-order ME effect, which occurs in the absence of magnetic order, can be expressed as

$$P^k = \beta_{ij}^k H_i H_j, \quad (i, j, k = x, y \text{ or } z). \tag{1}$$

Here, β_{ij}^k is the second-order ME susceptibility, which is a third-rank polar tensor, and $\boldsymbol{H}$ is the magnetic field. The first observation of the $\boldsymbol{P}$ by the second-order ME effect was reported for the non-centrosymmetric transition metal complex $NiSO_4 \cdot 6H_2O$ [12]. Importantly, the origin of the second-order ME effect in $NiSO_4 \cdot 6H_2O$ has been identified to be the p–d hybridization. The maximum value of P in this compound is limited to 18 $\mu C/m^2$ [12,16]. Subsequently, the second-order ME effect was observed in several compounds such as $CsCuCl_3$ and $HoAl_3(BO_3)_4$ [15,18,19]. The maximum value of P in the former is 0.4 $\mu C/m^2$, whereas $P \sim 3600$ $\mu C/m^2$, which was suggested to be caused by atomic displacement due to magnetostriction, was reported for the latter. However, the JT-driven second-order ME effect has not been identified yet. This Letter reports and explains it for the first time.

The transition metal complex [Mn^{III}(taa)] {H_3taa = tris[1-(2-azolyl)-2-azabuten-4-yl]amine} with no magnetic order at any temperature is a $3d^4$ spin-crossover (SCO)

complex [20–29], which exhibits an abrupt spin conversion between the high-spin (HS) state with $S = 2$ and the low-spin (LS) state with $S = 1$ at $T_{SCO} \sim 47$ K. [Mn^{III}(taa)] belongs to the cubic space group $I\bar{4}3d$, whose point group is piezoelectric $\bar{4}3m$ [20], allowing the occurrence of the second-order ME effect. An important feature of [Mn^{III}(taa)] is that the dynamic JT effect appears in its HS state, reflecting the C_3 symmetry of the molecule [22–26,29]. Because the twofold degeneracy of the e_g orbitals remains under the C_3 symmetry, JT instability arises in the HS state of [Mn^{III}(taa)], where only one electron occupies the e_g orbitals, thereby causing spontaneous molecular distortion. Density functional theory (DFT) calculations have demonstrated molecular elongation along one of the coordination axes by JT distortion [23]. Reflecting C_3 symmetry, there are three equivalent directions of molecular elongation. The JT distortion in [Mn^{III}(taa)] is not ordered but dynamically reorients from one direction to the others and also generates an electric dipole. Thus, the dynamic JT effect is accompanied by a fluctuating electric dipole, which results in paraelectric behavior in the HS state [22,23]. It is noteworthy that the JT distortion can couple with a spin via spin-orbit interaction [30]. By treating the spin-orbit interaction as a second order perturbation, the effective spin Hamiltonian for a Mn^{III} ion under the distorted ligand field is expressed as $\mathcal{H} = DS_Z^2 - E(S_X^2 - S_Y^2)$, where Z is along the molecular elongation axis. From the previous electron spin resonance (ESR) measurements, D/k_B and E/k_B were evaluated to be -8.49 and 0.72 K, respectively, in the HS state of [Mn^{III}(taa)] [29]. A negative D implies that the molecular elongation due to the JT distortion tends to align parallel to the spin. Therefore, the alignment of spins by the applied magnetic field is considered to cause an alignment of the molecular elongations, resulting in the alignment of the electric dipoles generated by the JT distortion. From the paraelectric Curie-Weiss behavior in the dielectric constant in [Mn^{III}(taa)], it is evaluated that a fluctuating electric dipole moment of 1.25D is generated by the JT distortion for a molecule [23]. This value is more than 100 times larger than the electric polarization induced by the spin current mechanism for a Mn atom in the representative ME multiferroic $TbMnO_3$ [31]. We consider that the induction of macroscopic electric polarization owing to the second-order ME effect is caused by the alignment of these large electric dipoles by the magnetic field. Thus, we expect a strong enhancement of the second-order ME effect by the dynamic JT effect in [Mn^{III}(taa)].

In this Letter, we observed magnetic-field-induced electric polarization 1 order larger than that of $NiSO_4 \cdot 6H_2O$ in the HS state of [Mn^{III}(taa)]. The value of the observed electric polarization is explained by our calculation, which takes into account the alignment of the JT distortion by the magnetic field under the influence of the spin-orbit interaction.

[Mn^{III}(taa)], which belongs to the $\bar{4}3m$ point group, has nonzero components of the third-rank polar tensor $\beta_{yz}^x = \beta_{zx}^y = \beta_{xy}^z = \beta$ [32]. Therefore, the electric polarization P^z induced by the second-order ME effect is expressed as

$$P^z = \beta(H_x H_y + H_y H_x) = \beta H^2 \sin(2\theta). \tag{2}$$

Here, z is parallel to [001], and θ is the angle between the [100] axis and the magnetic field, which is applied in the (001) plane. To observe P^z, we measured the displacement current induced by the change in P^z under rotating magnetic fields. A single crystal of [Mn^{III}(taa)] was prepared using the method described by Sim and Sinn [20]. The displacement current was measured in the temperature T range of 40 to 80 K in magnetic fields up to 17.5 T by using a KEITHLEY 6517B electrometer. P^z was evaluated from the time integral of the displacement current. A silver paste (Du Pont, 4922N) was used as the electrode on the sample to measure the displacement current along the [001]. A magnetic field was applied to the (001) plane. The sample was rotated in a magnetic field at 36°/min in the displacement current measurements.

Figures 1(a) and 1(b) show the field evolution of the angular dependence of the electric polarization P^z at 50 K and the temperature evolution of the P^z in the magnetic field of 17.5 T, respectively. The sinusoidal angular dependence of P^z with a 180° period was observed, which is in agreement with Eq. (2). Weak oscillations of the data with a period of approximately 14°, resulted from inevitable background signals of the measurement system. This oscillations appears even in zero magnetic field and thus is suspected to be due to slight mechanical vibration of the rotating system. Figures 1(c) and 1(d) show the magnetic field and temperature dependences, respectively, of P^z for $\boldsymbol{H}//[110]$ ($\theta = 45°$). The P^z at 50 K increases almost proportionally to the square of the magnetic field with $\beta = 0.152 \pm 0.0015\ \mu C/m^2\ T^2$, as shown in the inset in Fig. 1(c). This behavior unambiguously indicates that the observed P^z originates from the second-order ME effect. As shown in Fig. 1(d), P^z increases on cooling and reaches over 100 $\mu C/m^2$ at 43.7 K. This value is 1 order of magnitude larger than the maximum polarization in $NiSO_4 \cdot 6H_2O$ [16]. As the temperature is further decreased, P^z abruptly decreases to almost zero below 43 K, at which [Mn^{III}(taa)] undergoes the SCO transition to the LS state with no JT effect. Therefore, the observed P^z originates from the electric dipole generated by the JT effect on the molecule. The temperature dependence of P^z is proportional to $(T - \theta_W)^{-2}$ with the Weiss temperature $\theta_W = 31.5 \pm 0.25$ K, obtained from the fitting of the data as shown in the dashed curve in Fig. 1(d). Therefore, P^z is enhanced by the ferrodistortive interaction between the JT-distorted [Mn^{III}(taa)] molecules. The above results show

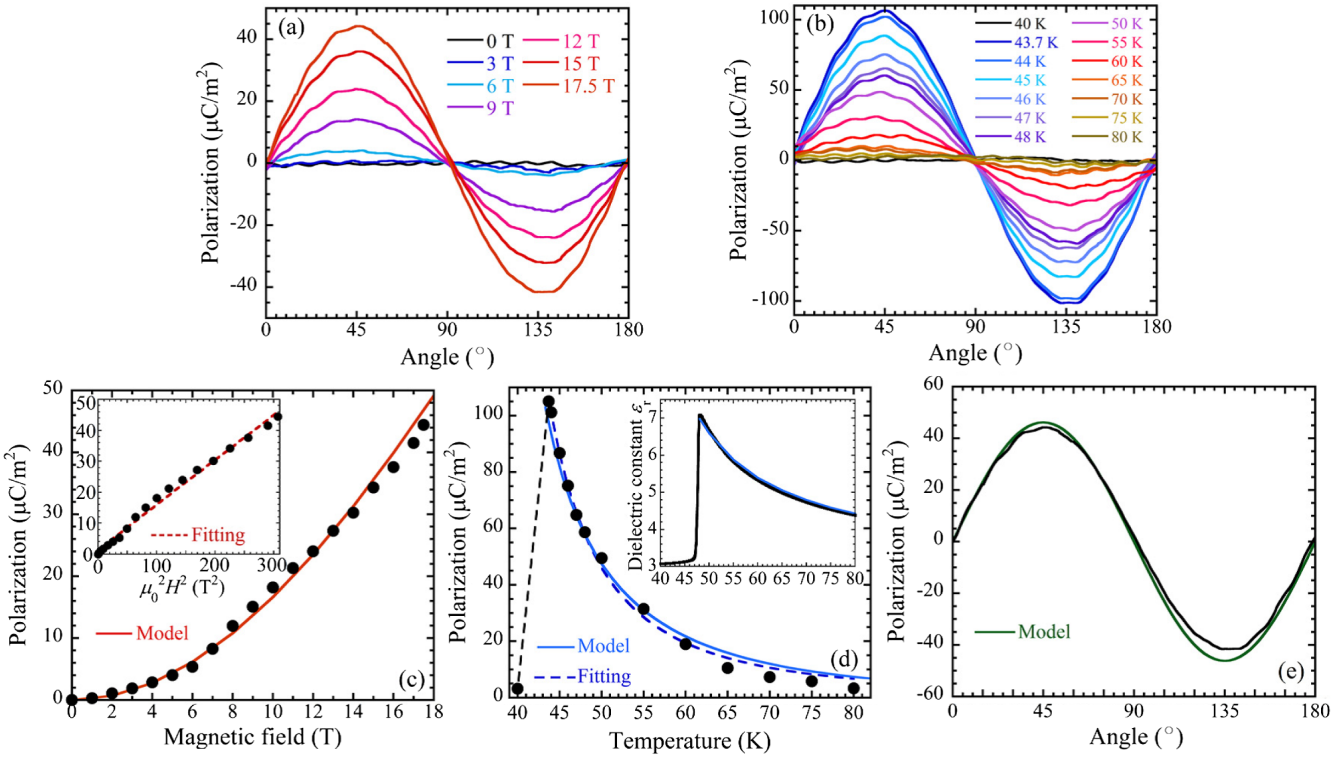

FIG. 1. (a) Field and (b) temperature evolutions of the angular dependence of the electric polarization P^z. The former is measured at 50 K and the latter is at 17.5 T. (c) Magnetic field dependence of the P^z at 50 K. The inset shows the P^z vs $\mu_0^2H^2$. The dashed line is a linear fit with $\beta = 0.152\ \mu\mathrm{C/m^2\ T^2}$. (d) Temperature dependence of the P^z at 17.5 T under cooling. The inset shows the temperature dependence of the dielectric constant ε_r under warming. (e) Angular dependence of the P^z at 50 K and 17.5 T. The closed circle and the black curves are the experimental results. The red, blue, and green solid curves show the calculated results. A constant $\varepsilon_\infty = 3.0$ is added to the calculated ε_r.

that the ME effect in [Mn^{III}(taa)] is considerably enhanced owing to the alignment of the JT distortion by the magnetic field, as expected.

The observed P^z values are examined by microscopic calculation, considering the alignment of the JT distortion by the magnetic field under the influence of the spin-orbit interaction. Figure 2(a) shows the averaged structure of the MnN_6 octahedron in a [Mn^{III}(taa)] molecule determined by the x-ray diffraction [20]. The MnN_6 octahedron is drawn by VESTA 3 [33]. The two equilateral triangles composed of the N(1) and N(7) atoms are twisted by 50.8° to each other around the C_3 axis penetrating the Mn^{III} ion. As a result, the directions of the Mn–N(1) and Mn–N(7) bonds are slightly inclined from the principal axes of the crystal. Owing to the JT distortion, a pair of the Mn–N(1) and Mn–N(7) bonds are elongated, while the remaining four

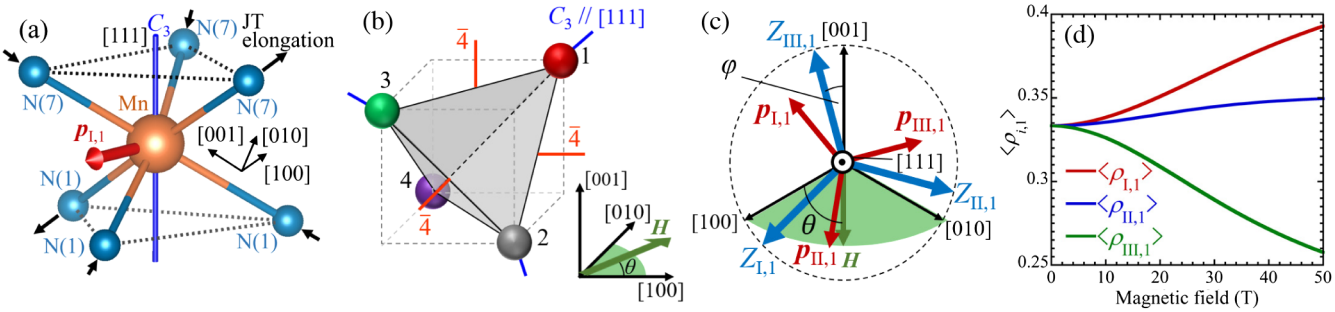

FIG. 2. (a) Averaged structure of the MnN_6 octahedron belonging to the sublattice 1 [33] and the electric dipole $\boldsymbol{p}_{I,1}$. (b) A regular tetrahedron, which represents a $\bar{4}3m$ point group. The C_3 axes of the molecules on the sublattices 1–4 are transferred to each other by $\bar{4}$ operations along the principal axes. The magnetic field is applied in the (001) plane. (c) The directions of the principal axes $Z_{i,1}$, (i = I, II, and III) of the magnetic anisotropy, and the electric dipoles $\boldsymbol{p}_{i,1}$ for a molecule belonging to the sublattice 1. (d) Magnetic field dependence of occupation probability $\langle\rho_{i,1}\rangle$, calculated for $\boldsymbol{H}//[110]$ at 50 K.

Mn–N bonds shrink [23], thereby generating an electric dipole in the molecule. Although the electric dipole has components both parallel and perpendicular to the molecular C_3 axis, only the perpendicular one contributes to the electric polarization induced by $\boldsymbol{H}$ because the parallel ones, induced by the three different JT distortions, are the same as each other and thus are not affected by $\boldsymbol{H}$.

The unit cell of [Mn^{III}(taa)] contains the 16 molecules, of which Mn^{III} ions are located on the 16c sites [20,23]. These 16 molecules are grouped into four sublattices, $n = 1$–4, whose C_3 axes align toward the four body diagonal directions of the cubic unit cell. Reflecting the $\bar{4}3m$ symmetry, the directions of the C_3 axes are transferred to each other by $\bar{4}$ operations along the principal axes. The arrangements of the molecules in the unit cell can be represented by a regular tetrahedron with four Mn^{III} ions on its corners, as shown in Fig. 2(b). When the magnetic dipoles along the [100] are induced at the each Mn^{III} ion by the magnetic field for $\boldsymbol{H}//[100]$, the magnetic point group of the tetrahedron is $\bar{4}2'm'$ without polarity. Therefore, the appearance of $\boldsymbol{P}$ is prohibited for $\boldsymbol{H}//[100]$. In contrast, the induction of $\boldsymbol{P}//[001]$ is allowed for $\boldsymbol{H}//[110]$, as we observed, because the magnetic point group becomes polar $2'mm'$.

The symmetry condition indicates that the macroscopic electric polarization perpendicular to [001] is not induced by the field in the (001) plane. Therefore, we calculated the [001] component of the electric polarization P^z, which is expressed as $P^z = 4N\sum_{n=1}^{4}\langle p_n^z\rangle$. Here, N is the total number of unit cells and $\langle p_n^z\rangle$ is electric dipole induced on a molecule belonging to sublattice $n = 1$–4. Thus, we first calculated p_1^z on the sublattice 1, in which the C_3 axis is directed along the [111] direction, as shown in Fig. 2(b). The bond elongations because of the JT distortion cause the aforementioned single-ion-type magnetic anisotropy with a negative D term. As shown in Fig. 2(c), the direction of the principal Z_i ($i = $ I, II, or III) axis of the magnetic anisotropy is considered to be inclined from the principal axes of the crystal by an angle φ around the [111] axis of the unit cell because of the slight inclination of the Mn–N bonds. Here, $i = $ I, II, or III represent the three molecular distorted states by the JT effect. Reflecting the C_3 symmetry, the directions of Z_i change by 120° to each other around the [111] direction. Neglecting the small rhombic E term, the spin Hamiltonian for the ith distorted state is expressed as $\mathcal{H}_{S,i} = -g\mu_B\boldsymbol{S}\cdot\boldsymbol{H} + DS_{Z_i}^2$. Here, $D/k_B = -8.49$ K, $g = 2.0$ the g factor [29], and μ_B the Bohr magneton.

The ferrodistortive interaction between the molecules, as indicated by the positive Weiss temperature [22,23], is represented by a 3-state Potts model $\mathcal{H}_F = J\sum_{i=\mathrm{I,II,III}}\rho_{i,1}^2$. Here, $J < 0$ is the ferrodistortive interaction constant, and the $\rho_{i,1}$ is the population of the ith state with $\rho_{i,1} = 1$ or 0. Treating the $\mathcal{H}_F$ by molecular field approximation, the occupation probability $\langle\rho_{i,1}\rangle$ of the ith distorted state is obtained by $\langle\rho_{i,1}\rangle = f_{i,1}/\sum_{i=\mathrm{I,II,III}} f_{i,1}$ with

$$f_{i,1} = e^{\frac{-J\langle\rho_{i,1}\rangle}{k_BT}}\sum_{\alpha=1}^{5} e^{\frac{-E_{i,1}^{\alpha}}{k_BT}}. \tag{3}$$

Here, $E_{i,1}^{\alpha}$ the eigenenergy of the $\mathcal{H}_{S,i}$, $\alpha = 1$–5 five eigenstates for $S = 2$, k_B the Boltzmann constant. Then, the electric polarization $\langle p_1^z\rangle$ along [001] induced by the magnetic field on the molecule is given as $\langle p_1^z\rangle = \sum_{i=\mathrm{I,II,III}} p_{i,1}^z\langle\rho_{i,1}\rangle$, where $p_{i,1}^z$ is the z component of the electric dipole $\boldsymbol{p}_{i,1}$ perpendicular to the C_3 axis, induced by the JT distortion. The $\boldsymbol{p}_{i,1}$ lies in a plane comprising two elongated Mn–N bonds. Thus, the direction of $\boldsymbol{p}_{i,1}$ could be obtained from the atomic positions of Mn, N(1), and N(7), as determined by previous x-ray diffraction measurements [20]. The absolute value of 1.25D of the electric dipole, obtained from the Curie constant $C = 91$ K [23], was used for the calculation. The electric polarization $\langle p_n^z\rangle$, ($n = 2$–4) was also calculated by a similar procedure by transferring the directions of $Z_{i,1}$ and $\boldsymbol{p}_{i,1}$ by the $\bar{4}$ operations. The solid curves in Figs. 1(c), 1(d), and 1(e) show the theoretical total electric polarization $P^z = 4N\sum_{n=1}^{4}\langle p_n^z\rangle$, and Fig. 2(d) shows the magnetic field dependence of the $\langle\rho_{i,1}\rangle$ for $\boldsymbol{H}//[110]$ at 50 K, numerically calculated with $J = -90$ K and $\varphi = 6.45°$. The values of the J is evaluated to reproduce the temperature dependence of the dielectric constant shown in the inset in Fig. 1(d), and the φ is determined so as to explain the magnetic field dependence of P^z at 50 K. As shown in Fig. 2(d), the $\langle\rho_{\mathrm{I},1}\rangle$ dominantly increases with increasing the magnetic field because the direction of the $Z_{\mathrm{I},1}$ is closer to the [110] compared to these of the $Z_{\mathrm{II},1}$ and $Z_{\mathrm{III},1}$. This result demonstrates the alignment of the molecular distortion by magnetic fields. The calculated P^z values in Fig. 1 successfully explain the overall results of the experiments, namely, the magnetic field, temperature, and sinusoidal angular dependences of P^z.

Finally, we discuss a recent report on the appearance of electric polarization by magnetic field-induced spin crossover from the LS to HS state [34,35]. It was suggested that this electric polarization is induced by the structural transition to a polar state with the frozen JT electric dipole. In fact, a large electric polarization parallel to H, prohibited for the second-order ME effect in the $\bar{4}3m$ system, was reported. Thus, the origin of this electric polarization seems to be different from the second-order ME effect. On the other hand, the temperature dependence of P^z with a finite Weiss temperature in Fig. 1(d) implies that some second-order structural phase transition occurs at temperature $T_c \sim \theta_W = 31.5$ K owing to the ferrodistortive intermolecular interaction. The high-field experimental result that the electric polarization in the field-induced HS state is considerably decreased below approximately 29 K [34] suggests that the nonpolar structure is below T_c. Therefore, we consider that the lowest temperature field-induced HS phase probably belongs to a nonpolar tetragonal $\bar{4}2m$ point group.

In conclusion, the enhancement of the second-order ME effect owing to the alignment of the dynamic JT distortion by the magnetic field was observed for the first time. High flexibility of the dynamic JT distortion, which responds to the external magnetic field in the paramagnetic state, enables this enhancement of the ME effect. The electric polarization reaches 100 $\mu C/m^2$, which is 1 order of magnitude larger than what originates from the p–d hybridization [12,16]. Although this value is smaller than the electric polarization induced by the spin-driven ferroelectricity in $TbMnO_3$ at ambient pressure, the electric polarization of 1.6×10^{-2} D per Mn^{III} ion in [Mn^{III}(taa)] is larger than that of 1.4×10^{-2} D in $TbMnO_3$ [31]. For the dynamic JT system with stronger spin-orbit interaction and a denser concentration of magnetic ions, a further increase in the electric polarization can be expected. Our calculation demonstrated that because of the coupling between the JT distortion and the spin via the spin-orbit interaction, the JT electric dipoles are aligned by the magnetic field, thereby inducing a large macroscopic electric polarization. This procedure for enhancing the ME effect can potentially enable new method for the practical use of the ME effect.

The authors thank Professor M. Matsumoto and Professor M. Koga for their valuable discussions. The experiments were performed in the GIMRT proposal, Institute for Materials Research, Tohoku University (No. 20H0415 and No. 202012-HMKGE-0405). This work was partially supported by the Grant-in-Aid for Scientific Research (Grants No. 19H01834 and No. 21H01026) from MEXT Japan and the Grant Fund for Research and Education of Institute for Materials Research, Tohoku University (No. J190001231).

[1] Y. Tokura, S. Seki, and N. Nagaosa, Multiferroics of spin origin, Rep. Prog. Phys. **77**, 076501 (2014).
[2] J. M. Hu and C. W. Nan, Opportunities and challenges for magnetoelectric devices, APL Mater. **7**, 080905 (2019).
[3] H. Katsura, N. Nagaosa, and A. V. Balatsky, Spin Current and Magnetoelectric Effect in Noncollinear Magnets, Phys. Rev. Lett. **95**, 057205 (2005).
[4] C. Jia, S. Onoda, N. Nagaosa, and J. H. Ham, Microscopic theory of spin-polarization coupling in multiferroic transition metal oxides, Phys. Rev. B **76**, 144424 (2007).
[5] T. Arima, Ferroelectricity induced by proper-screw type magnetic order, J. Phys. Soc. Jpn. **76**, 073702 (2007).
[6] I. A. Sergienko, C. Şen, and E. Dagotto, Ferroelectricity in the Magnetic E-Phase of Orthorhombic Perovskites, Phys. Rev. Lett. **97**, 227204 (2006).
[7] V. Y. Pomjakushin, M. Kenzelmann, A. Dönni, A. B. Harris, T. Nakajima, S. Mitsuda, M. Tachibana, L. Keller, J. Mesot, H. Kitazawa, and E. Takayama-Muromachi, Evidence for large electric polarization from collinear magnetism in $TmMnO_3$, New J. Phys. **11**, 043019 (2009).
[8] T. Aoyama, K. Yamauchi, A. Iyama, S. Picozzi, K. Shimizu, and T. Kimura, Giant spin-driven ferroelectric polarization in $TbMnO_3$ under high pressure, Nat. Commun. **5**, 4927 (2014).
[9] T. Aoyama, A. Iyama, K. Shimizu, and T. Kimura, Multiferroicity in orthorhombic $RMnO_3$ (R = Dy,Tb, and Gd) under high pressure, Phys. Rev. B **91**, 081107(R) (2015).
[10] P. Barone, K. Yamauchi, and S. Picozzi, Jahn-Teller distortions as a novel source of multiferroicity, Phys. Rev. B **92**, 014116 (2015).
[11] M. Lee, Q. Chen, E. S. Choi, Q. Huang, Z. Wang, L. Ling, Z. Qu, G. H. Wang, J. Ma, A. A. Aczel, and H. D. Zhou, Magnetoelectric effect arising from a field-induced pseudo Jahn-Teller distortion in a rare-earth magnet, Phys. Rev. Mater. **4**, 094411 (2020).
[12] S. L. Hou and N. Bloembergen, Paramagnetoelectric Effects in $NiSO_4 \cdot 6H_2O$, Phys. Rev. **138**, A1218 (1965).
[13] E. Ascher, Higher-order magneto-electric effects, Philos. Mag. **17**, 149 (1968).
[14] R. P. Chaudhury, B. Lorenz, Y. Y. Sun, L. N. Bezmaternykh, V. L. Temerov, and C. W. Chu, Magnetoelectricity and magnetostriction due to the rare-earth moment in $TmAl_3(BO_3)_4$, Phys. Rev. B **81**, 220402(R) (2010).
[15] K.-C. Liang, R. P. Chaudhury, B. Lorenz, Y. Y. Sun, L. N. Bezmaternykh, V. L. Temerov, and C. W. Chu, Giant magnetoelectric effect in $HoAl_3(BO_3)_4$, Phys. Rev. B **83**, 180417(R) (2011).
[16] A. I. Kharkovskiy, Y. V. Shaldin, and V. I. Nizhankovskii, Magnetoelectric effect and magnetostriction in the paramagnetic piezoelectric $NiSO_4 \cdot 6H_2O$, J. Exp. Theor. Phys. **117**, 1071 (2013).
[17] M. Akaki, H. Iwamoto, T. Kihara, M. Tokunaga, and H. Kuwahara, Multiferroic properties of an åkermanite $Sr_2CoSi_2O_7$ single crystal in high magnetic fields, Phys. Rev. B **86**, 060413(R) (2012).
[18] A. Miyake, J. Shibuya, M. Akaki, H. Tanaka, and M. Tokunaga, Magnetic field induced polar phase in the chiral magnet $CsCuCl_3$, Phys. Rev. B **92**, 100406(R) (2015).
[19] A. I. Kharkovskiy, Y. V. Shaldin, and V. I. Nizhankovskii, Nonlinear magnetoelectric effect and magnetostriction in piezoelectric $CsCuCl_3$ in paramagnetic and antiferromagnetic states, J. Appl. Phys. **119**, 014101 (2016).
[20] P. G. Sim and E. Sinn, First manganese(III) spin crossover, first d^4 crossover. Comment on cytochrome oxidase, J. Am. Chem. Soc. **103**, 241 (1981).
[21] Y. Garcia, O. Kahn, J. P. Ader, A. Buzdin, Y. Meurdesoif, and M. Guillot, The effect of a magnetic field on the inversion temperature of a spin crossover compound revisited, Phys. Lett. A **271**, 145 (2000).
[22] M. Nakano, G. E. Matsubayashi, and T. Matsuo, Dielectric behavior of manganese(III) spin-crossover complex [Mn(taa)], Phys. Rev. B **66**, 212412 (2002).
[23] M. Nakano, G. Matsubayashi, and T. Matsuo, Dynamic Jahn–Teller Character of Manganese(III) Spin-Crossover Complex [Mn(taa)] (H_3taa = tris(1-(2-azolyl)-2-azabuten-4-yl)amine), Adv. Quantum Chem. **44**, 617 (2003).
[24] S. Kimura, Y. Narumi, K. Kindo, M. Nakano, and G.-e. Matsubayashi, Field-induced spin-crossover transition of [Mn^{III}(taa)] studied under pulsed magnetic fields, Phys. Rev. B **72**, 064448 (2005).
[25] P. Guionneau, M. Marchivie, Y. Garcia, J. A. K. Howard, and D. Chasseau, Spin crossover in [Mn^{III}(pyrol)3tren]

probed by high-pressure and low-temperature x-ray diffraction, Phys. Rev. B **72**, 214408 (2005).

[26] Y. Sawada, S. Kimura, K. Watanabe, and M. Nakano, High-Field Optical Spectroscopy of the Spin-Crossover Complex [Mn^{III}(taa)], J. Low Temp. Phys. **170**, 424 (2013).

[27] K. Ridier, S. Petit, B. Gillon, G. Chaboussant, D. A. Safin, and Y. Garcia, Magnetic neutron spectroscopy of a spin-transition Mn3+ molecular complex, Phys. Rev. B **90**, 104407 (2014).

[28] Y. Otsuki, S. Kimura, S. Awaji, and M. Nakano, Magneto-capacitance effect and magnetostriction by the field-induced spin-crossover in [Mn^{III}(taa)], AIP Adv. **9**, 085219 (2019).

[29] S. Kimura, T. Otani, Y. Narumi, K. Kindo, M. Nakano, and G. Matsubayashi, ESR study of spin-crossover complex [Mn^{III}(taa)] using pulsed high magnetic field, J. Magn. Magn. Mater. **272–276**, 1102 (2004).

[30] S. Ohtani, Y. Watanabe, M. Saito, N. Abe, K. Taniguchi, H. Sagayama, T. Arima, M. Watanabe, and Y. Noda, Orbital dilution effect in ferrimagnetic $Fe_{1-x}Mn_xCr_2O_4$: competition between anharmonic lattice potential and spin–orbit coupling, J. Phys. Condens. Matter **22**, 176003 (2010).

[31] T. Kimura, T. Goto, H. Shintani, K. Ishizaka, T. Arima, and Y. Tokura, Magnetic control of ferroelectric polarization, Nature (London) **426**, 55 (2003).

[32] J. F. Nye, *Physical Properties of Crystals* (Oxford University Press, Oxford, 1957).

[33] K. Momma and F. Izumi, VESTA 3 for three-dimensional visualization of crystal, volumetric and morphology data, J. Appl. Crystallogr. **44**, 1272 (2011).

[34] S. Chikara, J. Gu, X.-G. Zhang, H.-P. Cheng, N. Smythe, J. Singleton, B. Scott, E. Krenkel, J. Eckert, and V. S. Zapf, Magnetoelectric behavior via a spin state transition, Nat. Commun. **10**, 4043 (2019).

[35] J.-X. Yu, D.-T. Chen, J. Gu, J. Chen, J. Jiang, L. Zhang, Y. Yu, X.-G. Zhang, V. S. Zapf, and H.-P. Cheng, Three Jahn-Teller States of Matter in Spin-Crossover System Mn(taa), Phys. Rev. Lett. **124**, 227201 (2020).